J. Fluid Mech. (1970), *vol.* 42, *part* 3, *pp.* 433–446
Printed in Great Britain

A free-streamline model of the two-dimensional sail

By J. P. DUGAN
University of Toronto

(Received 27 October 1969 and in revised form 12 January 1970)

The two-dimensional sail is considered in a free-streamline model to complement the oft-considered airfoil model which is limited to small angles of attack. The shape of the sail, the lift and drag coefficients, and the moment are obtained for various angles of attack and states of tension.

1. Introduction

The sailboat is an intriguing device long used by man in his livelihood and recreation. The sail, as the motive power for the boat, has been the object of much interest. Although there have been several attempts by fluid mechanicians over the years to model the sail analytically, most efforts to quantitatively evaluate its efficiency have been experimental (cf. Shenstone 1968). Probably the most interesting experiment, by which to obtain the efficiency of the sail set at different trim, is to measure the speed of one's own boat. Evidently, the efficiency of the sail is increased if the boat moves faster. There seems to be little doubt that this is the best way to design a sail (Marchaj 1964; Letcher 1965). However, to model a sail analytically presents a challenge that, in the end, could increase our knowledge of its workings.

The first model of a sail seems to be that of Cisotti (1932). This is a free-streamline model in which the flow separates at the edges of the sail, forming an infinite quiescent wake. Since Cisotti did not exhibit any results, his model is used here to determine the shape and the lift and drag coefficients of an idealized sail. This model is essentially different from the more recent aerodynamic models chosen by Voelz (1950) and Thwaites (1961). In these papers, the sail is replaced by a linear distribution of vortices just as is done in airfoil theory, with the exception of the change in the boundary condition. Voelz (1950) obtained the sail shape and the first eigenvalue of the linear integral equation for the strength of the vortex sheet. The solution for values of the parameter that are less than this eigenvalue is shown to be the usual concave shape expected of a sail. Somewhat surprisingly, however, the solution for values of the parameter greater than the eigenvalue showed an inflexion of the sail profile. Thwaites (1961), apparently unaware of the earlier work, covered some of the same ground and he showed the existence of higher eigenvalues, each one determining the onset of a higher mode of the sail shape. These papers also exhibit lift coefficients. Chambers (1966) confirmed the earlier numerical estimates of the eigenvalues by a variational procedure and Nielsen (1963), choosing to formulate the problem

in terms of airfoil camber and a differential equation for the aerodynamic loading of the sail instead of in an integral equation, obtained equivalent results. Nielsen (1963) also performed experiments on a flexible sail in a wind tunnel and, although the results shown are sketchy, a comment on the possible importance of the porosity of the sail fabric apparently stimulated an analysis of the effects of porosity by Barakat (1968).

The airfoil theory predicts some interesting characteristics of sails. Probably the most important is the existence of inflexion points in the profile when the tension is not too great. That theory is, however, limited to very small angles of attack (ones smaller than those usually found on boats) and it predicts zero drag. The model used here eliminates these difficulties, but it does still treat only two-dimensional sails, and it does have physical limitations of its own. For example, the free-streamline theory in the simple form used here predicts a wake of infinite length. One does find a long wake in practice as every sailor knows when he is 'covered', but it does not extend to infinity. Also, as used in practice, the sail is seldom fully 'stalled', that is, only partial separation occurs. Finally, this model still leaves out all effects of viscosity and turbulence.

This formulation, then, based on Cisotti's model, uses the conformal mapping technique of Levi-Civita (1907) as modified by Villat (1911) and as discussed by Birkhoff & Zarantonello (1957). Thus, the particulars are somewhat different from those of Cisotti. The resulting non-linear, singular integral equation has been solved for asymptotically small deflexion of the sail for the special case of a symmetric sail (Dugan 1966). Here, it is solved asymptotically for small deflexion, and solved numerically to obtain the sail and free streamline profiles and the drag, lift and moment experienced by the sail.

2. Formulation

The representation of incompressible, two-dimensional potential motion can be formulated in the complex notation,

$$\left.\begin{aligned} Z &= X+iY = L^{-1}(x+i\psi), \\ W &= \Phi+i\Psi = U^{-1}L^{-1}(\phi+i\psi), \\ \zeta &= U^{-1}(u-iv) = U^{-1}\frac{dw}{dz} = \frac{dW}{dZ}, \end{aligned}\right\} \tag{1}$$

where U is the uniform fluid velocity at infinity, L is the length of the sail, small-lettered variables are dimensional, and capital lettered ones non-dimensional. The co-ordinate system and appropriate variables are shown in figure 1. The boundary conditions are that the velocity is uniform at infinity, the pressure is continuous across the free streamlines, and the pressure difference across the sail is balanced by the tension along the sail. The first and second boundary conditions give

$$\tfrac{1}{2}\rho U^2|\zeta|^2+P = \tfrac{1}{2}\rho U^2+P_0 = \text{const.}, \tag{2}$$

where P_0 is the pressure in the quiescent wake. This gives the condition,

$$|\zeta|^2 = 1 \quad \text{on} \quad AJ_1 \quad \text{and} \quad BJ_2, \tag{3}$$

the free streamlines. A force balance on a differential element of the sail as shown in figure 2 gives

$$(P - P_0)\, dl \cos(d\beta) = T \sin(d\beta), \tag{4}$$

where dl is the differential arc length and $d\beta$ is the differential angle of deflexion of the element. The tension T is assumed to be constant and the sail to be inextensible. Since $d\beta$ is small, (2) and (4) give

$$T\frac{d\beta}{dl} = \tfrac{1}{2}\rho U^2(1 - |\zeta|^2), \tag{5}$$

as the boundary condition on the sail.

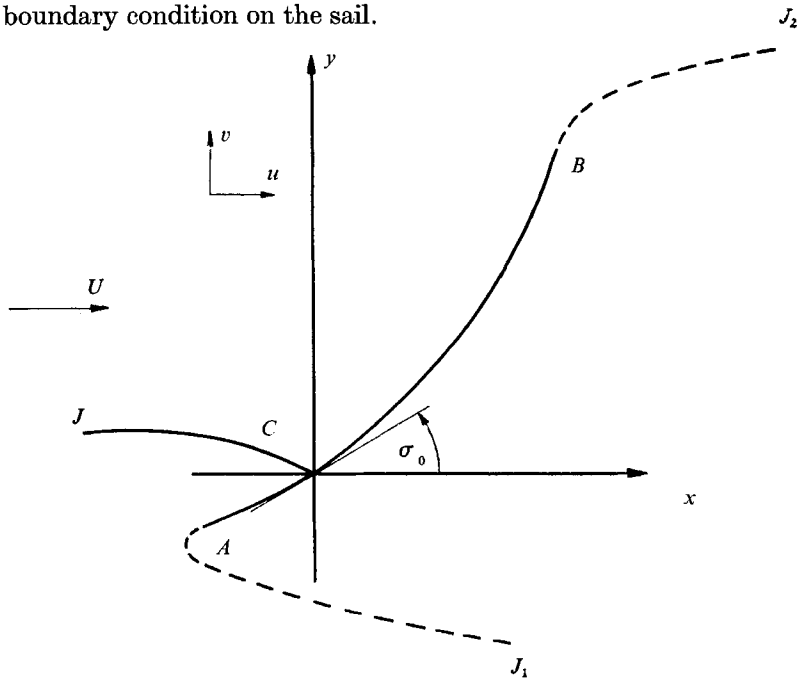

FIGURE 1. The physical z-plane.

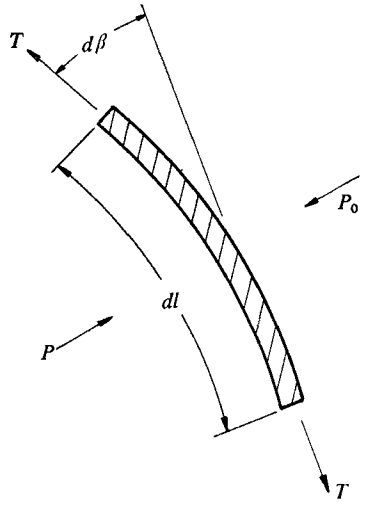

FIGURE 2. Force balance on an element of the sail.

If one could directly obtain the mapping of the W-plane into the Z-plane the problem would be simple indeed. However, this is not practically possible so it is convenient to utilize the technique of Levi-Civita (1907) as modified by Villat (1911). This method consists of mapping the W-plane into an auxiliary t-plane and finding an analytic function Ω, called the Levi-Civita function, that maps the t-plane into the ζ-plane where it is possible to apply the boundary conditions. The t-plane contains the flow field in the interior of a semi-circle, the circumference

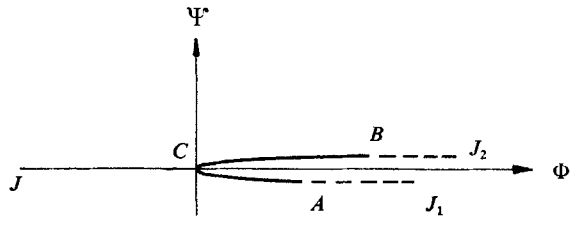

W-plane

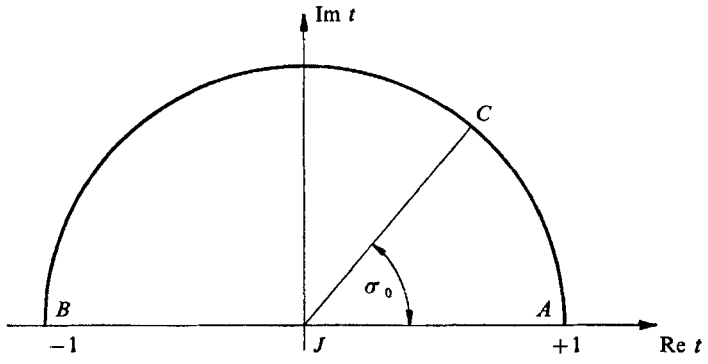

t-plane

FIGURE 3. Auxiliary complex planes.

of which corresponds to the sail and the diameter of which corresponds to the free streamlines. A functional relation involving the Levi-Civita function is assumed between the ζ- and t-planes. This functional relation, once Ω is computed, completes the connexion between the W- and ζ-planes.

The W-plane is mapped into the t-plane by the transformation,

$$W = M[\cos\sigma_0 - \tfrac{1}{2}(t + t^{-1})]^2, \tag{6}$$

as shown in figure 3. M is an unknown constant introduced in the normalization of the semi-circle and reflects the fact that the separation points A and B cannot be explicitly located in the W-plane. An integral relation for M will be derived

later. The functional relation between the t- and ζ-planes is assumed to be of the form,

$$\zeta(t) = \frac{t - e^{i\sigma_0}}{1 - t\,e^{i\sigma_0}} e^{i(\pi - \sigma_0)} e^{-i\Omega(t)}. \tag{7}$$

The Levi-Civita function Ω is a complex quantity in general, and it may be written

$$\Omega = \theta + i\tau. \tag{8}$$

This particular form for the relation between the ζ- and t-planes is chosen because it immediately allows Ω to be single-valued and continuous in t and it allows automatic satisfaction of one of the boundary conditions. The choice is really fixed by the solution of the corresponding flat plate problem.

Thus, since the free streamlines correspond to the interval $(-1, 1)$ of the real line in the t-plane, the requirement,

$$t = \alpha, \quad -1 \leqslant \alpha \leqslant 1,$$

gives

$$|\zeta| = \left|\frac{\alpha - e^{i\sigma_0}}{1 - \alpha\, e^{i\sigma_0}}\right| \; \left| e^{i(\pi - \sigma_0)} e^{\tau} e^{-i\theta} \right| = e^{\tau}. \tag{9}$$

With (3), this gives

$$\tau = 0 \quad \text{on} \quad -1 \leqslant \operatorname{Re} t \leqslant 1. \tag{10}$$

Therefore, requiring Ω to be real on the real line will satisfy this boundary condition automatically. Also, the sail corresponds to

$$t = e^{i\sigma} \quad (0 \leqslant \sigma \leqslant \pi),$$

so that

$$\arg \zeta = \begin{cases} -\sigma_0 - \theta + \pi & \text{on} \quad 0 \leqslant \sigma < \sigma_0, \\ -\sigma_0 - \theta & \text{on} \quad \sigma_0 < \sigma \leqslant \pi. \end{cases} \tag{11}$$

Due to the form of (7), then, the fluid velocity has a jump in its argument of π radians at the stagnation point σ_0, as it should from physical reasoning. This allows Ω to be single-valued and continuous everywhere in the interior of the t-plane.

It remains to use these expressions to obtain Ω. A simple construction (Birkhoff & Zarantonello 1957, p. 134, or Dugan 1966, p. 11) shows that

$$\sigma_0 + \theta = \beta,$$

or

$$d\theta = d\beta,$$

so that (5) can be written as

$$\frac{d\theta}{d\sigma} = \frac{\rho U^2}{2T}(1 - |\zeta|^2)\frac{dl}{d\sigma}. \tag{12}$$

Geometric arguments give

$$dl = L|dZ|,$$

and this, with (1), yields

$$\frac{dl}{d\sigma} = L|\zeta^{-1}| \left|\frac{dW}{dt}\right| \left|\frac{dt}{d\sigma}\right|,$$

so that on $t = e^{i\sigma}$, and with (6) and (7),

$$\frac{d\theta}{d\sigma} = 2MK \sin\sigma \{\sin\sigma \sin\sigma_0 \cosh\tau(\sigma) - (1 - \cos\sigma \cos\sigma_0)\sinh\tau(\sigma)\} \quad (0 \leqslant \sigma \leqslant \pi), \tag{13}$$

where

$$K = \frac{\rho U^2 L}{2T}.$$

Recapitulating, (13) is a relation between θ and τ, the real and imaginary parts of the Levi-Civita function. It represents the boundary condition on the sail.

The Levi-Civita function may be extended to an analytic function in the unit circle $|t| \leqslant 1$, so that the series

$$\Omega(t) = \sum_{n=0}^{\infty} a_n t^n \tag{14}$$

exists. The a_n's must all be real constants by (10) (the boundary condition on the free streamlines), so that, with (8),

$$\left.\begin{aligned} \theta(\sigma) &= \sum_{n=0}^{\infty} a_n \cos n\sigma, \\ \tau(\sigma) &= \sum_{n=0}^{\infty} a_n \sin n\sigma, \end{aligned}\right\} \quad \text{on} \quad t = e^{i\sigma} \quad (0 \leqslant \sigma \leqslant \pi). \tag{15}$$

Since both expressions contain the same constants, this constitutes a second relation between θ and τ. This relationship may be written in the more convenient form

$$\tau(\sigma) = \int_0^{\pi} D(\sigma, \sigma') \frac{d\theta}{d\sigma'} d\sigma',$$

$$\text{where} \quad D(\sigma, \sigma') = -\frac{2}{\pi} \sum_{j=1}^{\infty} \frac{\sin j\sigma \sin j\sigma'}{j} = -\frac{1}{\pi} \ln \left| \frac{\sin \frac{1}{2}(\sigma + \sigma')}{\sin \frac{1}{2}(\sigma - \sigma')} \right|. \tag{16}$$

(cf. Birkhoff & Zarantonello 1957, p. 136, or Dugan 1966, appendix IB). The substitution of (13) into the integral expression (16) gives

$$\tau(\sigma) = -\frac{2}{\pi} MK \int_0^{\pi} \ln \left| \frac{\sin \frac{1}{2}(\sigma + \sigma')}{\sin \frac{1}{2}(\sigma - \sigma')} \right| \sin \sigma' \{ \sin \sigma' \sin \sigma_0 \cosh \tau(\sigma') - (1 - \cos \sigma' \cos \sigma_0) \sinh \tau(\sigma') \} d\sigma' \quad (0 \leqslant \sigma \leqslant \pi). \tag{17}$$

This is a non-linear, singular integral equation for the imaginary part of the Levi-Civita function. Once $\tau(\sigma)$ is determined, $\Omega(t)$ can be constructed by obtaining the coefficients of the power series (14). However, there still remains in the integral equation the unknown constant M that was introduced in the conformal mapping.

This constant can be determined from the side condition (that has not been used up to now) that the total length of the sail is L. Using the geometric argument before (13),

$$dl = L|dZ| = L|\zeta^{-1}| \left| \frac{dW}{dt} \right| \left| \frac{dt}{d\sigma} \right| d\sigma,$$

and, substituting from above,

$$dl = 2ML \sin \sigma [1 - \cos (\sigma + \sigma_0)] e^{-\tau(\sigma)} d\sigma,$$

so that, upon integration, the side condition on M is

$$M = \left\{ 2 \int_0^{\pi} \sin \sigma [1 - \cos (\sigma + \sigma_0)] e^{-\tau(\sigma)} d\sigma \right\}^{-1}. \tag{18}$$

This relation, along with the integral equation (17) suffices to determine $\tau(\sigma)$.

The sail and free streamline profiles are obtained through (1)

$$dZ = \zeta^{-1}dW = \zeta^{-1}(t)\frac{dW}{dt}dt,$$

so that, substituting again from above,

$$dZ = -\frac{1-te^{i\sigma_0}}{t-e^{i\sigma_0}}e^{i(\sigma_0-\pi)}e^{i\Omega(t)}M[\cos\sigma_0-\tfrac{1}{2}(t+t^{-1})][1-t^{-2}]dt. \tag{19}$$

The parametric equations of the sail profile are obtained by substituting $t = e^{i\sigma}$ into this expression and integrating from the stagnation point C to the ends of the sail, that is, from $t = e^{i\sigma_0}$ to $t = 1$ or -1. The equations are

$$\hat{Z} = 2M\int_{\sigma_0}^{\sigma}\sin\sigma'[1-\cos(\sigma'+\sigma_0)]\,e^{i(\sigma_0+\theta(\sigma'))}e^{-\tau(\sigma')}d\sigma', \tag{20}$$

where $\hat{Z} = \hat{X}+i\hat{Y}$ denotes the co-ordinates of the sail profile. The equations of the free streamline profiles are obtained by substituting $t = \alpha$ where α is real into (19), and integrating from the ends of the sail to infinity, that is, from $t = 1$ or $t = -1$ to $t = 0$. In this case, the equations are

$$Z-\hat{Z}_T = \tfrac{1}{2}M\int_{\pm1}^{\alpha}\alpha'^{-3}(1-\alpha'^2)\,[2\alpha'-(1+\alpha'^2)\cos\sigma_0 + i(1-\alpha'^2)\sin\sigma_0]e^{i(\sigma_0+\theta(\alpha'))}d\alpha', \tag{21}$$

where $\hat{Z}-\hat{Z}_T = (\hat{X}-\hat{X}_T)+i(\hat{Y}-\hat{Y}_T)$ denotes the co-ordinates of the profiles and $\hat{Z}_T = \hat{X}_T+i\hat{Y}_T$ denotes the co-ordinates of the ends of the sail.

Just as for the profiles, the forces acting on the sail can be obtained by quadratures. Thus, a simple derivation gives

$$d\mathbf{F} = -i(P-P_0)\,dz,$$

so that

$$\mathbf{F} = -\tfrac{1}{2}i\rho U^2L\int_0^{\pi}(1-|\zeta|^2)\,\zeta^{-1}(e^{i\sigma})\frac{dW}{dt}\frac{dt}{d\sigma}d\sigma$$

or,

$$\mathbf{F} = -2iM\rho U^2L\int_0^{\pi}\{\sin\sigma\sin\sigma_0\cosh\tau(\sigma) - (1-\cos\sigma\cos\sigma_0)\sinh\tau(\sigma)\}e^{i\sigma_0}e^{i\theta(\sigma)}\sin\sigma\,d\sigma. \tag{22}$$

It is easily shown that $F_y = 0$ for $\sigma_0 = \frac{1}{2}\pi$ and that with

$$\mathbf{F} = F_x+iF_y = \tfrac{1}{2}\rho U^2L(C_D+iC_L),$$

$$C_D = \frac{2\pi\sin^2\sigma_0}{4+\pi\sin\sigma_0}, \quad C_L = -\frac{2\pi\sin\sigma_0\cos\sigma_0}{4+\pi\sin\sigma_0}$$

in the limit of $K \to 0$ of (22). These are the results for the flat plate. The drag and lift could have been obtained through the elegant formulae of Levi-Civita (see Gurevich 1966, p. 98) instead of through the integral (22). Similarly, the moment is given by

$$\mathbf{M} = \mathrm{Re}\{-\tfrac{1}{2}\rho U^2\textstyle\int z\zeta^2\,dz\}, \tag{23}$$

or

$$\mathbf{M} = -\rho U^2L^2M\int_0^{\pi}[1-\cos(\sigma-\sigma_0)]\,e^{\tau(\sigma)}\sin\sigma \times\{\hat{X}(\sigma)\cos(\sigma_0+\theta(\sigma))+\hat{Y}(\sigma)\sin(\sigma_0+\theta(\sigma))\}d\sigma, \tag{24}$$

where $\hat{X}(\sigma)$ and $\hat{Y}(\sigma)$ are given by (20).

3. Solution of equations and results

The determination of the sail profile and the forces and moment acting on the sail rests upon the solution of (17) for $\tau(\sigma)$. The equation is solved below by an asymptotic technique for small deflexion of the sail and by a numerical technique for arbitrary deflexions.

The limit $K \to 0$ (this may be interpreted as $T \to \infty$) reduces the problem to the flat-plate problem considered by Rayleigh (1876). Equation (17) gives $\tau(\sigma) = 0$ so, by expressions (15), $\theta(\sigma) = 0$. Evidently, then, $\tau(\sigma)$ and $\theta(\sigma)$ are small for small deflexions of the sail ($K \ll 1$). In fact, the form of (17) implies that MK is an appropriate perturbation parameter so that it is natural to assume a solution of the form,

$$\tau(\sigma) = \tau_0(\sigma) + MK\tau_1(\sigma) + (MK)^2\tau_2(\sigma) + \ldots, \tag{25}$$

for $MK \ll 1$. Actually, (17) also implies that $\tau(\sigma) \leqslant 0$, so (18) yields

$$M \leqslant (4 + \pi \sin\sigma_0)^{-1} \leqslant \tfrac{1}{4}, \tag{26}$$

verifying that $MK \ll 1$ if $K \ll 1$. Substituting the expansion (25) into (17), expanding the hyperbolic functions, and equating coefficients of equal powers in MK gives the sequence of equations,

$$\left.\begin{aligned}
&\tau_0(\sigma) = 0,\\
&\tau_1(\sigma) = -4\pi^{-1}\sin\sigma_0 \int_0^\pi D(\sigma,\sigma')\sin\sigma'\,d\sigma',\\
&\tau_2(\sigma) = 4\pi^{-1}\int_0^\pi D(\sigma,\sigma')(1-\cos\sigma_0\cos\sigma')\tau_1(\sigma')\,d\sigma',\\
&\tau_3(\sigma) = -4\pi^{-1}\int_0^\pi D(\sigma,\sigma^1)\{2^{-1}\tau_1^2(\sigma')\sin\sigma_0\sin\sigma' - (1-\cos\sigma_0\cos\sigma')\tau_2(\sigma')\}\,d\sigma',\\
&\quad\vdots
\end{aligned}\right\} \tag{27}$$

where $D(\sigma,\sigma')$ is the former of the two kernel functions (16). Evaluation of these integrals gives

$$\left.\begin{aligned}
\tau_1(\sigma) &= 16\pi^{-1}\sin\sigma_0 \sum_{n=1}^{\infty} \frac{\sin(2n-1)\sigma}{(2n-1)^2[(2n-1)^2-4]},\\
\tau_2(\sigma) &= -256\pi^{-2}\sin\sigma_0 \sum_{j,n=1}^{\infty} \{(2j-1)[(2j-1)^2-4]\}^{-1}\\
&\quad\times\left\{\frac{\sin(2n-1)\sigma}{[(2n-1)^2-4(j-1)^2][(2n-1)^2-4j^2]} - \frac{\cos\sigma_0\cos 2n\sigma}{[4n^2-(2j-3)^2][4n^2-(2j+1)^2]}\right\}.\\
&\quad\vdots
\end{aligned}\right\} \tag{28}$$

The next correction $\tau_3(\sigma)$ has been computed, but it is quite messy and is not of sufficient interest to include here. The corresponding values of the constant M can be obtained by substituting the expansion (25) and (28) into (18), so that

$$M = (4+\pi\sin\sigma_0)^{-1}\left\{1 - K\frac{16}{3\pi}\sin\sigma_0\frac{\pi+2\sin\sigma_0}{(4+\pi\sin\sigma_0)^2} + O(K^2)\right\}. \tag{29}$$

The resulting three-term approximate expression for $\tau(\sigma)$ appears to converge for values of K up to unity; the two-term expansion for values up to about one-half. It is of more than passing interest to note that the first two terms above are identical to the first two terms of the Neumann series solution of the linearized form of (17). The non-linearity of (17) and, therefore, the non-linearity of the boundary condition on the sail becomes important when $K \gtrsim \frac{1}{2}$ since that is when the third and higher order terms in the expansion (25) become important. The Neumann series solution mentioned above converges strictly for $MK < 3^{-\frac{1}{2}}$, the first eigenvalue of the homogeneous linearized equation (see Courant & Hilbert 1953, p. 153; Tricomi 1957, p. 50). In the limit $\sigma_0 \to 0$ and $K \ll 1$, (29) gives $M = 4^{-1}$, so that the expansion converges for $K \lesssim 2{\cdot}310$. Considering that this is only an approximate estimate of the limit of K in the linearized case of a completely different theory, it is remarkable that this value of K is so close to Voelz's (1950) first eigenvalue, 2·299 in the present notation, which was corrected by Thwaites (1961) and Chambers (1966) to 2·316. This limiting value of K has no bearing on the non-linear problem.

In the approximation above, the drag and lift coefficients (22) are given by

$$\mathbf{C} = \frac{2\pi \sin\sigma_0}{4+\pi\sin\sigma_0}(\sin\sigma_0 - i\cos\sigma_0)\left\{1+\frac{16}{3\pi}\frac{K}{4+\pi\sin\sigma_0} \times\left(1-\sin\sigma_0\frac{\pi+2\sin\sigma_0}{4+\pi\sin\sigma_0}\right)-O(K^2)\right\}. \quad (30)$$

The integral equation (17) with the side condition (18) also has been solved by successive approximations whereby, assuming an initial M_0 and $\tau_0(\sigma)$, corrections are found successively by the formulae

$$M_{n+1} = \left\{2\int_0^\pi \sin\sigma'[1-\cos(\sigma'+\sigma_0)]\,e^{\tau_n(\sigma')}d\sigma'\right\}^{-1}$$

and
$$\tau_{n+1}(\sigma) = 2M_{n+1}K\int_0^\pi D(\sigma,\sigma')\sin\sigma' \times\{\sin\sigma'\sin\sigma_0\cosh\tau_n(\sigma') - (1-\cos\sigma'\cos\sigma_0)\sinh\tau_n(\sigma')\}d\sigma', \quad (31)$$

where $D(\sigma,\sigma')$ is the second kernel function (16). The integrals are evaluated numerically by Simpson's rule, proper care being taken with the singularity. The details of this and the calculation of the remaining integrals do not seem worth repeating here, they are straight-forward and, in any case, they may be found in Dugan (1966). We note only that the solution of (31) above converges nicely ($|M_{n+1}-M_n| < 0{\cdot}0001$, $\max|\tau_{n+1}(\sigma)-\tau_n(\sigma)| < 0{\cdot}0001$) for $\sigma_0 \gtrsim 5°$, $K \lesssim 7$. Sample solutions for the sail profile are shown in figure 4 for several values of K and the angle of attack and, the lift and drag coefficients are plotted in figures 5 and 6. Figure 7 is a plot of the lift/drag coefficient and figure 8 shows the moment acting on the sail. It should be noted that the parameter σ_0 is the angle of attack of the 'equivalent' flat-plate problem. Since the positions of the endpoints $\hat{Z}_T$ of the sail vary with K as well as with σ_0, the real angle of attack (angle between a line joining the endpoints and the x-axis) can only be determined from the sail

profile. This is of minor importance but it does cause difficulty in an attempt to compare the resulting sail profiles with previously derived ones. In the figures, the angle of attack is the real angle of attack as defined above, not the angle of attack of the 'equivalent' flat-plate problem.

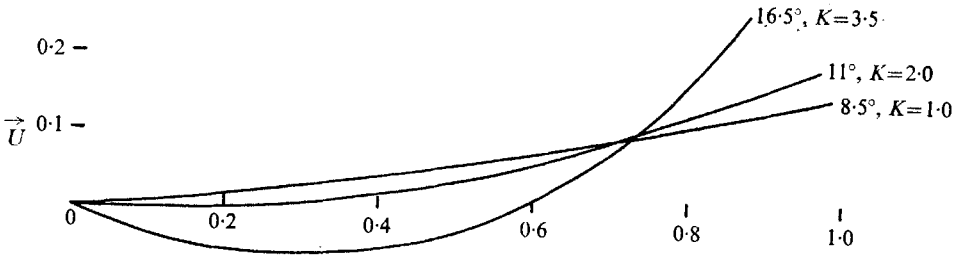

FIGURE 4. Sail profiles. In each case $\sigma_0 = 7{\cdot}5°$. Actual angle of attack = 8·5° for $K = 1$, 11° for $K = 2$, 16·5° for $K = 3{\cdot}5$.

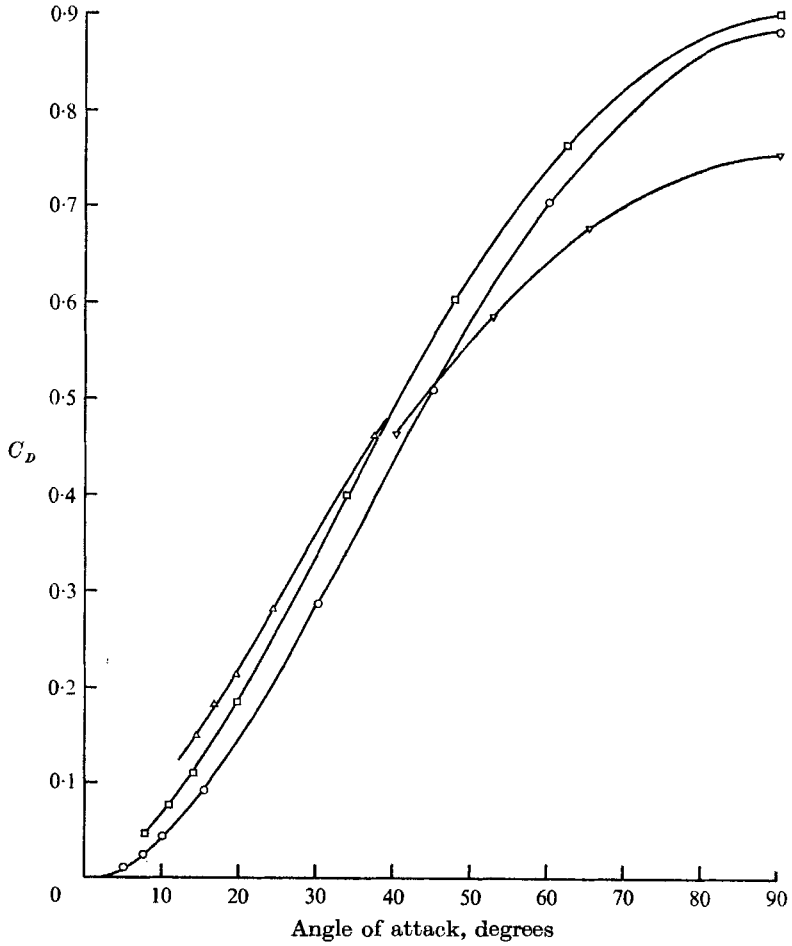

FIGURE 5. Plot of C_D *versus* angle of attack for various K. ○, $K = 0{\cdot}1$; △, $K = 3{\cdot}5$; □, $K = 2$; ▽, $K = 5$.

The lift and drag coefficients as defined in § 2 are proportional to those usually defined in airfoil theory except that the area is not the cross-sectional area but is the length L of the sail. The calculated drag coefficients are relatively independent of the parameter K, but the maximum lift coefficient increases markedly with increasing K, the maximum occurring at smaller angles of attack for larger values of K. This theory is invalid for zero angle of attack and this evidently

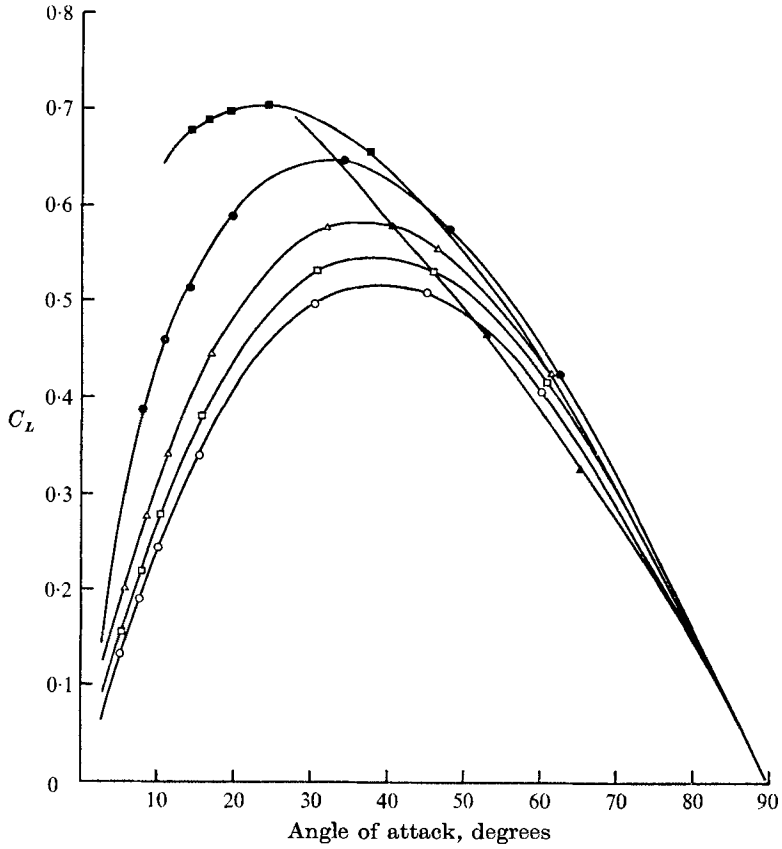

FIGURE 6. Plot of C_L *versus* angle of attack for various K. ○, $K = 0{\cdot}1$; □, $K = 0{\cdot}5$; △, $K = 1$; ●, $K = 2$; ■, $K = 3{\cdot}5$; ▲, $K = 5$.

appears in the difficulty in obtaining convergent solutions of the integral equations in this neighbourhood. However, the iterative scheme does converge for small angles of attack if K is small or moderate. The resulting lift coefficients which are plotted in figure 6 do not agree with those predicted by the airfoil analysis. The lift coefficient appears to increase linearly with the angle of attack for small angles but the limiting value is one-quarter the value predicted by Voelz (1950) and others. The disparity is embedded in the assumption that there is not separation in the airfoil theory while there is separation in the present case. However, since the experimental values of the lift coefficient obtained by Nielsen (1963) were one-half to one-third of those predicted by the airfoil theory, the

values predicted here in the limit of $\sigma_0 \to 0$ appear to be as valid as the previous ones. Figure 8 shows that the moment decreases with increasing values of K.

As mentioned above, this model breaks down when the angle of attack is too small. The tension in the sail has to be increased (K decreased), the smaller the

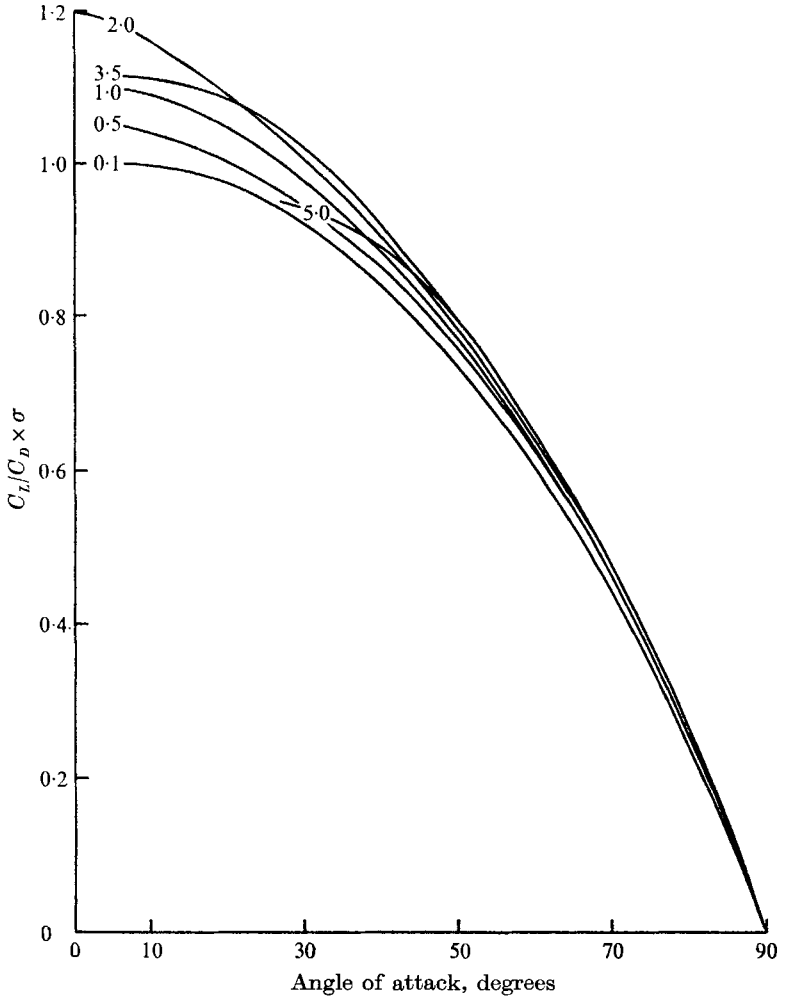

FIGURE 7. Plot of C_L/C_D times angle of attack *versus* angle of attack.

angle of attack, in order to obtain a convergent solution of (17). This is as might be expected physically, presumably foretelling the onset of a higher mode as predicted by the airfoil model.

In conclusion, then, the free-streamline model can be used to describe the aerodynamics of a two-dimensional sail. This model complements rather than supercedes the airfoil model because of different ranges of validity in the angle of attack. In the small range where each can predict solutions, this model should

be a better representation of reality because the stream would begin to separate from the back of the sail.

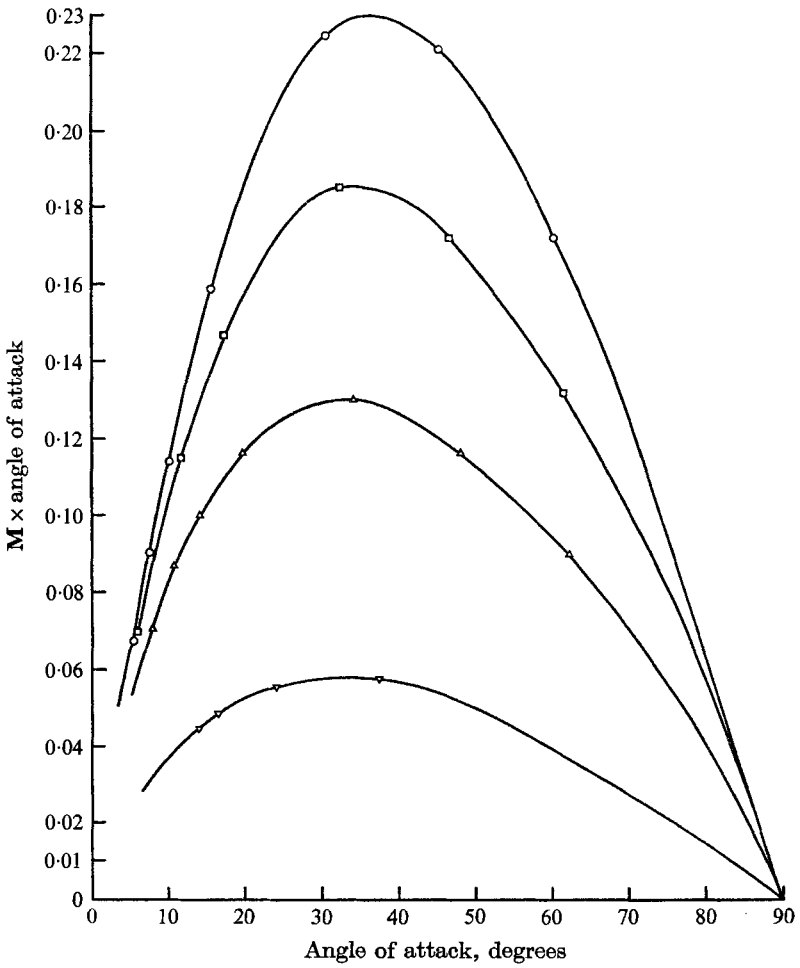

FIGURE 8. Plot of moment times angle of attack *versus* angle of attack. The moment = $\mathbf{M}.\rho U^2L^2$. ○, $K = 0{\cdot}1$; △, $K = 2$; □, $K = 1$; ▽, $K = 3{\cdot}5$.

It is a pleasure to thank W. E. Olmstead for his suggestion of this problem and his valuable guidance. A simpler version of the work made up an M.Sc. thesis submitted to Northwestern University, where the author was a NASA Fellow. Its final preparation was supported by NRC Grant A-7365.

REFERENCES

BARAKAT, R. 1968 Incompressible flow around porous two-dimensional sail and wings. *J. Math. Phys.* **47**, 327–349.

BIRKHOFF, G. & ZARANTONELLO, E. H. 1957 *Jets, Wakes and Cavities.* New York: Academic.

CHAMBERS, L. G. 1966 A variational formulation of the Thwaites sail equation. *Quart. J. Mech. Appl. Math.* **19**, 221–231.

CISOTTI, V. 1932 Moto con scia di un profilo flessibile, Nota I and II. *Rendiconti della reale Accad. Nat. dei Lincei* **15**, 166–173, 253–257.

COURANT, R. & HILBERT, D. 1953 *Methods of Mathematical Physics*, vol. 1. New York: Interscience.

DUGAN, J. P. 1966 Two-dimensional potential flow around a flexible membrane. M.S. Thesis, Northwestern University.

GUREVICH, M. I. 1966 *The Theory of Jets in an Ideal Fluid*. New York: Pergamon.

LETCHER, J. S. 1965 Balance of helm and static directional stability of yachts sailing close-hauled. *J. Roy. Aero. Soc.* **69**, 241–248.

LEVI-CIVITA, T. 1907 Scie e leggi di resistenzia. *Rend. Circolo Math. Palermo*, **23**, 1–37.

MARCHAJ, C. A. 1964 *Sailing Theory and Practice*. New York: Dodd-Mead.

NIELSEN, J. N. 1963 Theory of flexible aerodynamic surfaces. *J. Appl. Mech.* **30**, 435–442.

RAYLEIGH, LORD 1876 On the resistance of fluids. *Phil. Mag.* (5) **2**, 430–441.

SHENSTONE, B. S. 1968 Unconventional flight. *Aeronaut. J.* **72**, 655–666.

THWAITES, B. 1961 The aerodynamic theory of sails, I. Two-dimensional sails. *Proc. Roy. Soc.* A **261**, 402–422.

TRICOMI, F. G. 1957 *Integral Equations*. New York: Interscience.

VILLAT, H. 1911 Sur la résistance des fluides. *Ann. Sci. Ec. Norm.* **28**, 203–240.

VOELZ, K. 1950 Profil und Auftrieb eines Segels. *ZAMM* **30**, 301–317.